The Astrophysical Journal Letters, 721:L182–L188, 2010 October 1 doi:10.1088/2041-8205/721/2/L182

SEISMIC DIAGNOSTICS OF RED GIANTS: FIRST COMPARISON WITH STELLAR MODELS

J. Montalbán[1], A. Miglio[1,3], A. Noels[1], R. Scuflaire[1], and P. Ventura[2]
[1] Institut d'Astrophysique et Géophysique de l'Université de Liège, Allée du six Août, 17 B-4000 Liège, Belgium
[2] Osservatorio Astronomico di Roma-INAF, via Frascati 33, Monteporzio Catone, Rome, Italy
Received 2010 August 4; accepted 2010 August 28; published 2010 September 13

ABSTRACT

The clear detection with *CoRoT* and *KEPLER* of radial and non-radial solar-like oscillations in many red giants paves the way for seismic inferences on the structure of such stars. We present an overview of the properties of the adiabatic frequencies and frequency separations of radial and non-radial oscillation modes for an extended grid of models. We highlight how their detection allows a deeper insight into the internal structure and evolutionary state of red giants. In particular, we find that the properties of dipole modes constitute a promising seismic diagnostic tool of the evolutionary state of red giant stars. We compare our theoretical predictions with the first 34 days of *KEPLER* data and predict the frequency diagram expected for red giants in the *CoRoT* exofield in the galactic center direction.

Key words: stars: evolution – stars: interiors – stars: late-type – stars: oscillations

Online-only material: color figure

1. INTRODUCTION

Red giants are cool stars with an extended convective envelope, which can, as in main-sequence solar-like stars, stochastically excite pressure modes of oscillation. Although stochastic oscillations were already detected in a few red giants from ground- and space-based observations (e.g., Frandsen et al. 2002; De Ridder et al. 2006; Barban et al. 2007), it has been only through the photometric space mission *CoRoT* (Baglin et al. 2002) that an unambiguous detection of radial and non-radial modes in a large number of red giant stars has been achieved (De Ridder et al. 2009; Hekker et al. 2009; Carrier et al. 2010). That confirmation has opened the way to the seismic study of the structure and evolution of these objects that play a fundamental role in fields such as stellar age determination and chemical evolution of galaxies. The application of Kjeldsen & Bedding (1995) theoretical scaling laws, which relate basic seismic observables (the large frequency separation, $\Delta\nu$, and the frequency at maximum power, $\nu_{\rm max}$) to the stellar global parameters, allowed Mosser et al. (2010a) to estimate the masses of *CoRoT* and *KEPLER* red giants (adopting a value for the effective temperature). Moreover, the combination of these scalings with the predictions of population synthesis models let Miglio et al. (2009b) and Miglio et al. (2009a) to characterize the population of *CoRoT* and *KEPLER* targets.

These results showing that a vast amount of information can be extracted from quite easy-to-access seismic observables have deeply changed the perception of the predictive capabilities of asteroseismology and have strengthened its interaction with the other fields of astrophysics. However, much more information is contained in the oscillation spectra of this large number of red giants. In this Letter, we analyze the properties of red giant adiabatic oscillation spectra and relate them with their evolutionary state.

2. STELLAR MODELS

Stellar models were computed with the code ATON3.1 (Ventura et al. 2008, and references therein) for masses between 0.7 and 5.0 $M_\odot$, and different chemical compositions: He mass fraction, $Y = 0.25$ and 0.278, and metal mass fraction, $Z = 0.006$, 0.01, 0.015, 0.02, and 0.03. The energy transport in the convective regions was modeled with the classic mixing length treatment with $\alpha_{\rm MLT} = 1.6$. For a given chemical composition ($Z = 0.02$, $Y = 0.278$), models with $\alpha_{\rm MLT} = 1.9$ and FST (full spectrum of turbulence) treatment of convection (Canuto et al. 1996) were also computed. The evolution of these models was followed from the pre-main sequence until the exhaustion of He in the core for models more massive than 2.3 $M_\odot$ and until the helium flash for the less massive ones. The core He-burning (He-B) phase for low-mass (0.7–2.3 $M_\odot$) stars (red clump stars) has also been followed starting from zero-age horizontal branch models. Microscopic diffusion was not included but its effects on red giant models (Michaud et al. 2010) are not relevant for the present study.

The evolution rate during ascending red giant branch (RGB), descending RGB, and core He-B phases is very different and strongly depends on stellar mass. For low-mass stars, the time spent ascending the RGB may be comparable with that of core He burning of more massive stars. As a consequence, observing stars in both evolutionary stages would be equally likely. Concerning the internal structure of these models, it is worth mentioning that for a low-mass model (1.5 $M_\odot$, for instance) the density contrast ($\rho_c/\langle\rho\rangle$, central to mean density ratio) changes from 10^6 at the bottom of its RGB to 3×10^9 at $\log L/L_\odot \sim 2$. Models in the core He-B phase, on the other hand, have a much lower value of $\rho_c/\langle\rho\rangle$ of the order of 2×10^7; moreover, due to the high dependence on temperature of the 3α nuclear reactions, they develop a small convective core. At a given luminosity, e.g., that of the red clump, the value of $\rho_c/\langle\rho\rangle$ for a 1.5 $M_\odot$ RGB model is more than 10 times that of a He-B one. So different structures should imply significant effects on the oscillation properties.

3. ADIABATIC OSCILLATION PROPERTIES

Adiabatic oscillation frequencies were computed with an Eulerian version of the code LOSC (Scuflaire et al. 2008) for models from the bottom of the RGB up to a maximum luminosity ($\log L/L_\odot$ 2.2–3.2, depending on mass), as well during the

[3] Chargé de Recherches of the Fonds de la Recherche Scientifique, FNRS, rue d'Egmont 5, B-1000 Bruxelles, Belgium.

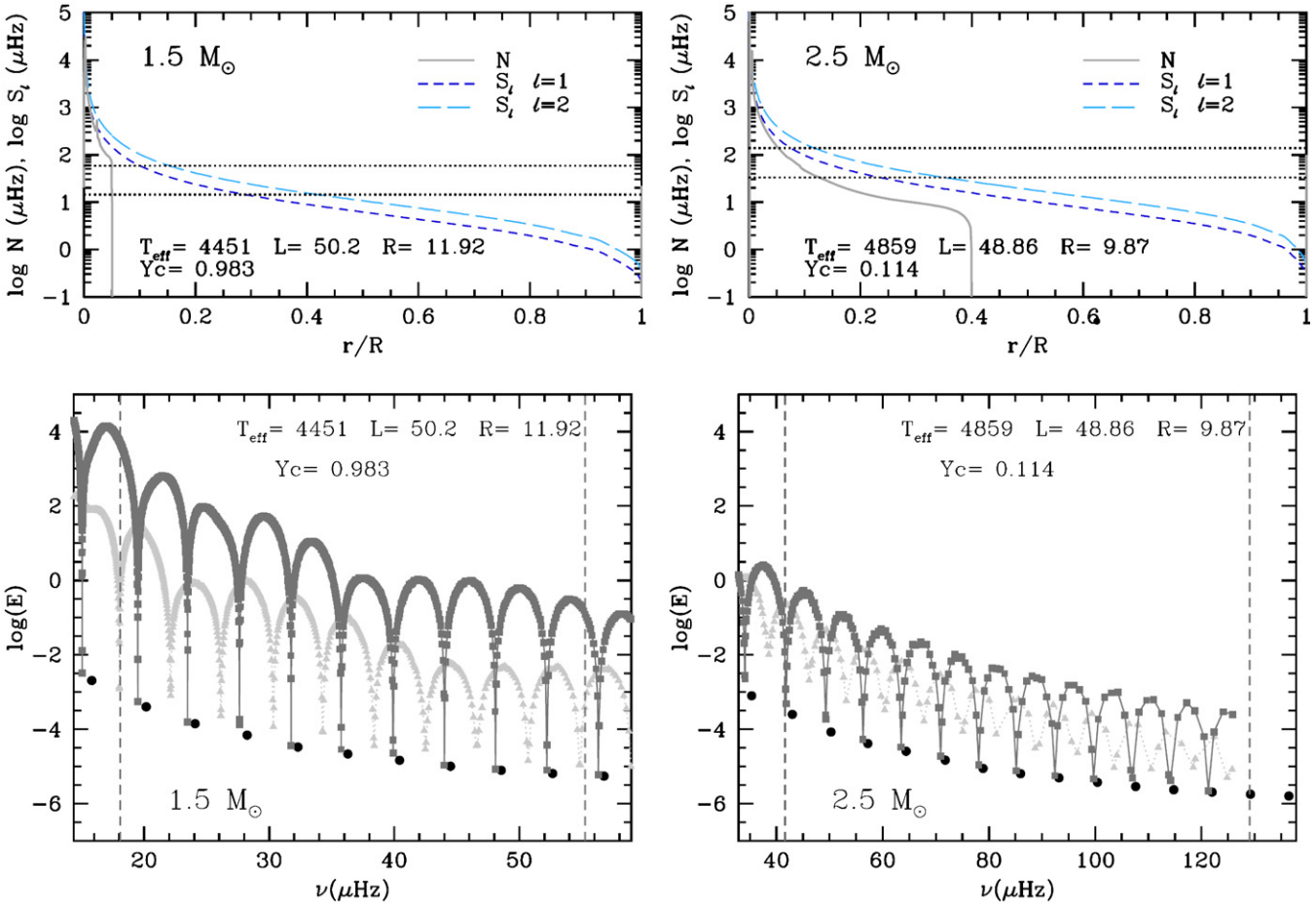

Figure 1. Upper panels: propagation diagrams for two models at almost the same luminosity, 1.5 $M_\odot$ in the RGB (left) and 2.5 $M_\odot$ in central He-burning (He-B) phase (right). Horizontal dotted lines limit the solar-like frequency domain for each model. Solid line is Brunt–Väisälä frequency, and short-dashed and long-dashed lines correspond to the Lamb frequency for $\ell = 1$ and 2, respectively. Lower panels: corresponding plots of inertia as a function of frequency for $\ell = 0$ (black circles), 1 (gray triangles), and 2 (dark gray squares) modes in the solar-like oscillation domain (dashed vertical lines).

(A color version of this figure is available in the online journal.)

phase of core He burning. In this Letter, we deal with adiabatic computations and do not consider the problem of excitation and damping of solar-like oscillations in red giants (Dziembowski et al. 2001; Houdek & Gough 2002; Dupret et al. 2009). We use the scaling laws (Brown et al. 1991; Kjeldsen & Bedding 1995) to derive the frequency domain in which solar-like oscillations are expected and the value of the mode inertia as an estimate of the expected mode amplitude (Christensen-Dalsgaard 2004). We search oscillation modes with angular degree $\ell = 0$, 1, 2, and 3[4] in the domain of frequencies defined by an interval around $\nu_{\max}$ (Equation (10) of Kjeldsen & Bedding 1995). The width of the solar-like frequency domain is taken to be 20% larger than the difference between the acoustic cutoff frequency in the stellar atmosphere and $\nu_{\max}$.

The properties of oscillation modes depend on the behavior of the Brunt–Väisälä (N) and Lamb (S_ℓ) frequencies. In red giant models, N reaches huge values in the central regions and therefore the frequency of gravity modes (g-modes) and their number by frequency interval (n_g) increase with respect to main-sequence models. On the other hand, the low mean density makes the frequency of pressure modes (p-modes) to decrease. All that leads to an oscillation spectrum for red giants where, in addition to radial modes, one finds a large number of non-radial modes with mixed g–p properties. The dominant character of these non-radial modes depends on the separation between gravity and acoustic cavities and may be estimated from the value of the normalized mode inertia (E; see, e.g., Christensen-Dalsgaard 2004, and references therein). Therefore, some non-radial modes may be well trapped in the acoustic cavity and behave as p-modes presenting a mode inertia close to that of radial modes, while modes with strong mixed g–p character have larger E value. Hereafter, we will use the term p-modes in quotation marks to refer to mixed modes with a dominant p-character.

In Figure 1, we present, in top panels, the $\ell = 1, 2$ propagation diagrams for an RGB 1.5 $M_\odot$ model (left) and for a core He-B model of 2.5 $M_\odot$ (right). In the bottom panels, we plot the variation of the mode inertia with frequency for radial and non-radial modes ($\ell = 1$, 2). As mentioned above, the RGB model is 10 times more centrally condensed than the He-B one. The huge difference in density between the central region and the convective envelope entails a high potential barrier between the acoustic and the gravity cavities reducing the interaction between p- and g-modes. As a consequence, we find for RGB models that $\ell = 1$ modes with $E_{\ell=1} \approx E_{\ell=0}$ are quite regularly spaced in frequency. For He-B ones, the coupling between these cavities is more important and $\ell = 1$ modes are mixed modes

[4] $\ell = 3$ only for $Z = 0.02$, $Y = 0.278$, and $\alpha_{\rm MLT} = 1.9$.

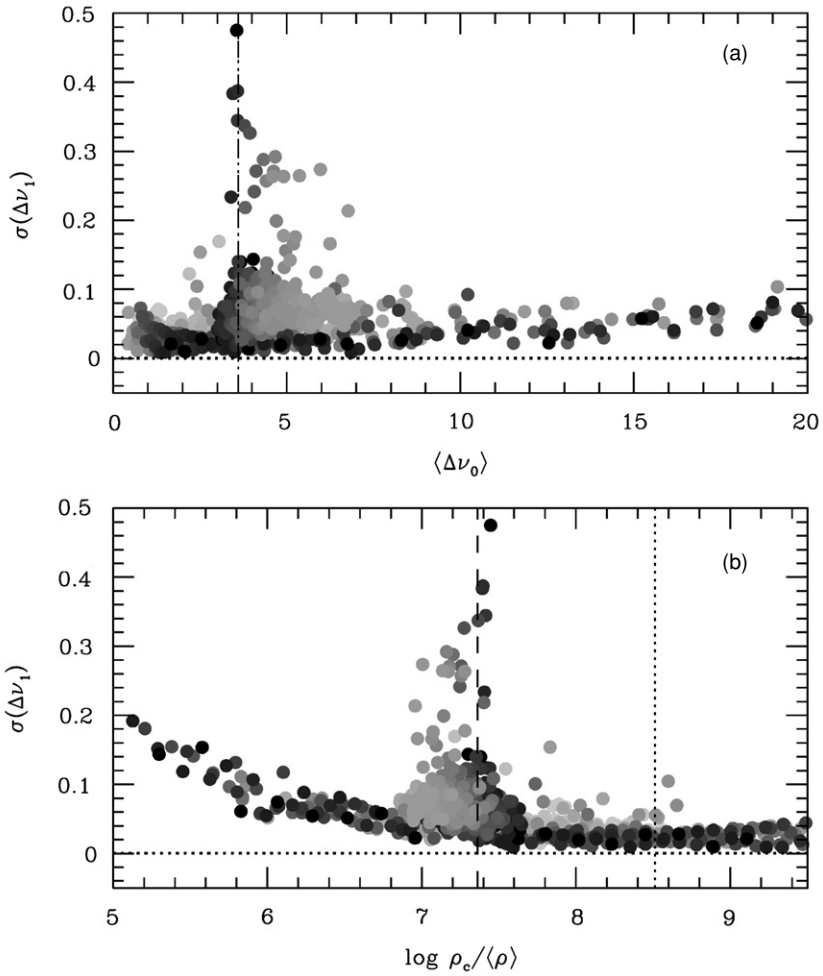

Figure 2. Mean squared deviation with respect to the main value of $\Delta\nu_{\ell=1}$, for RGB and core He-B models between 0.7 $M_\odot$ (darkest symbols) and 5.0 $M_\odot$ (lightest symbols), as a function of mean large separation for radial modes (a) and as a function of the density contrast (b). Vertical dotted and dashed lines correspond to 1 $M_\odot$ models at log $L/L_\odot \sim 1.68$ in the RGB and core He-B phases, respectively.

with $E_{\ell=1} > E_{\ell=0}$. Nevertheless, $E_{\ell=1}$ presents still a minimum value for modes between two consecutive radial ones showing a somewhat regular pattern. Even if the E value is larger than that corresponding to radial modes, we can still consider those modes, based on the value of E, as observable "p-modes." For $\ell = 2$ modes, the coupling between the g- and p-cavities is smaller than for $\ell = 1$, and hence the trapping is more efficient. Therefore, independently of the central condensation of the model, a spectrum of regularly spaced $\ell = 2$ "p-modes" with $E_{\ell=2} \approx E_{\ell=0}$ is expected. Finally, note that the turning points for acoustic modes (tp_ℓ defined as the point where $\nu_{\max} = S_\ell$) are inside the convective envelope for the RGB model and in the radiative region for the He-B one.

In the asymptotic theory for p-modes (Vandakurov 1967; Tassoul 1980; Gough 1986), the frequencies of two modes of same degree and consecutive order are separated by a constant value $\langle\Delta\nu\rangle$ which is approximately independent of ℓ for low-degree modes and related to the mean density of the star. Of course, the asymptotic theory is no longer valid for mixed modes and in regions with rapidly varying physical quantities, nevertheless, the modes partially or well trapped in the acoustic cavity with a dominant p-character ("p-modes") show such a regular pattern. We select then, as "p-modes" of degree ℓ, the modes with the minimum inertia between two consecutive radial modes and use them to compute the large and small frequency separations and to analyze their dependence on the stellar parameters and evolutionary state.

3.1. Large Separation: $\Delta\nu$

The mean value of the large frequency separation ($\langle\Delta\nu_\ell\rangle = \langle\nu_{n,\ell} - \nu_{n-1,\ell}\rangle$ averaged over the radial order n) decreases as the star ascends the RGB with a denser and denser core and a more and more diffuse envelope, but it is not possible to distinguish, on the basis of the $\langle\Delta\nu\rangle$ value alone, among different evolutionary states, ascending RGB, descending RGB, or core He burning. Nevertheless, an indirect information about the evolutionary state is provided not by the average value $\langle\Delta\nu\rangle$, but by the deviation of $\Delta\nu$ as a function of frequency with respect to its mean value ($\sigma(\Delta\nu_\ell)$). Radial and $\ell = 2$ "p-modes," as mentioned above, show a very regular pattern, and the mean quadratic deviation of $\Delta\nu(\nu)$ with respect to its mean value over the solar-like frequency domain ($\sigma(\Delta\nu_\ell)$) is always smaller than 5% for all the evolutionary states and masses considered. In contrast, $\sigma(\Delta\nu_1)$ strongly depends on the evolutionary state and while its value remains small for more concentrated models, it may get values as large as 50% for core He-B ones.

Figure 2 shows how the scatter of $\ell = 1$ modes depends on $\Delta\nu$ (that is on $\langle\rho\rangle$) and on the density contrast. The scatter of $\ell = 1$ frequencies decreases as the luminosity increases

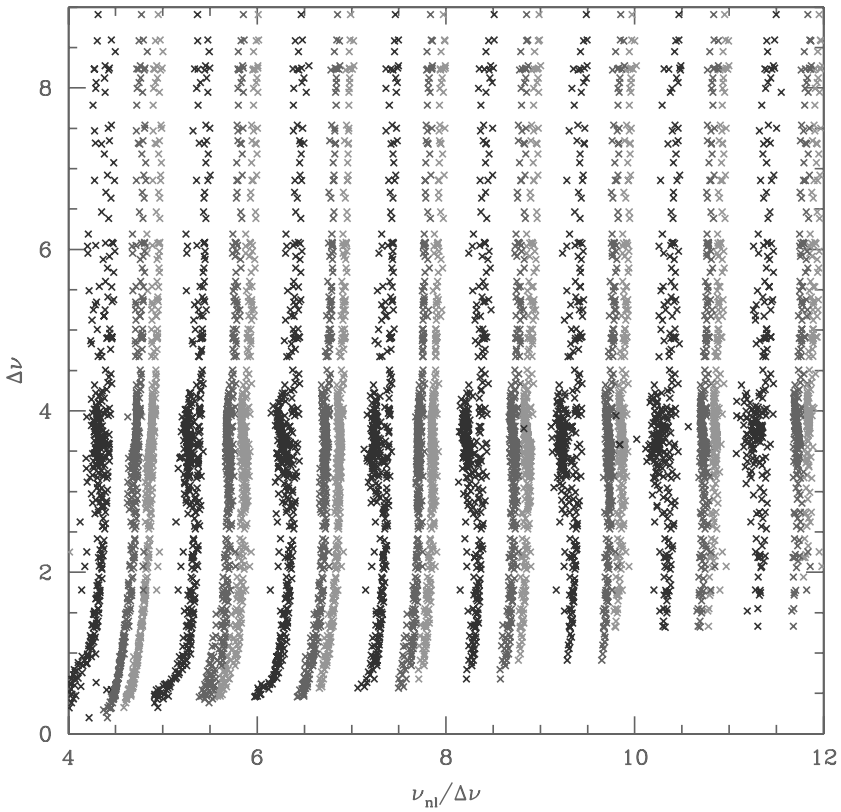

Figure 3. Theoretical oscillation pattern expected for $\ell = 0$ (light gray), 1 (black), and 2 (dark gray) modes from the red giant population in the *CoRoT* exofield in the galactic center direction. In ordinate the large frequency separation for radial modes and in abscissa the frequency of (n, ℓ) modes are normalized by the large separation.

from the bottom of the RGB (low $\rho_c/\langle\rho\rangle$, or highest $\langle\Delta\nu\rangle$). As the star goes up the RGB, the $\ell = 1$ modes are better trapped in the acoustic cavity and the spectra of dipole modes are more regular. These results are consistent with the observational results obtained by Bedding et al. (2010) for the first 34 days of *KEPLER* observations: radial and quadruple modes for a sample of 50 low luminosity red giants (<30 $L_\odot$ from scaling laws) show a low scatter, while dipole modes present a significantly larger one. The large dispersion shown in Figure 2 around $\langle\Delta\nu_0\rangle \sim 4\,\mu$Hz and $\rho_c/\langle\rho\rangle \sim 2 \times 10^7$ corresponds to models burning He in the core. Following the core expansion, the external convective zone recedes, increasing the coupling between gravity and acoustic cavities (see Figure 1) and the mixed character of oscillation modes. The spectrum of "trapped" $\ell = 1$ modes is then much less regular. It is worth pointing out that, for a given mass (1 $M_\odot$, for instance) at red clump luminosity, while RGB and core He-B models have the same value of $\langle\Delta\nu_0\rangle$, $\rho_c/\langle\rho\rangle$ may differ by two orders of magnitude.

The distributions of $\Delta\nu$ and $\nu_{\max}$ for the *CoRoT* exofield red giant sample show a single dominant peak located at ~4 μHz and ~30 μHz, respectively (Hekker et al. 2009), which was interpreted by Miglio et al. (2009b) as being consistent with a population of red giants dominated by red clump stars. According to population synthesis simulations done with TRILEGAL (Girardi et al. 2005) for the *CoRoT* field in the galactic center direction, 70% of the stars at the red clump luminosity are low-mass stars in the core He-B phase, and therefore, with oscillation spectra significantly different from those of the other 30% of stars that, at the same luminosity, are in the RGB phase. In Figure 3, we plot the "ensemble oscillation pattern" that we expect for the *CoRoT* red giant population in the galactic center direction. This diagram was obtained by taking the theoretical adiabatic spectra corresponding to the stellar models whose stellar parameters are closest to those resulting from population synthesis computations. Note the large scatter of $\ell = 1$ modes in the region around $\langle\Delta\nu\rangle \sim 4\,\mu$Hz and the regular pattern of $\ell = 0$ and 2 modes. Both characteristics are in good agreement with the observational results found by Mosser et al. (2010b).

3.2. Small Separations: $\delta\nu_{02}$, $\delta\nu_{03}$, and $\delta\nu_{01}$

According to the asymptotic theory, the mean small frequency separation ($\langle\delta\nu_{02}\rangle = \langle\nu_{n0} - \nu_{n-1\,2}\rangle$) is related to the behavior of the sound speed (c) mostly in the central regions, and hence to the stellar evolutionary state. The representation of $\langle\delta\nu_{02}\rangle$ versus $\langle\Delta\nu\rangle$ is in fact considered as a seismic diagnostic diagram allowing to derive stellar mass and age for main-sequence solar-like pulsators (Christensen-Dalsgaard 1988). The corresponding seismic diagram for red giant models is drawn in Figure 4(a) which shows a linear dependence of $\langle\delta\nu_{02}\rangle$ on $\langle\Delta\nu_0\rangle$, with a slope that increases as the mass decreases. In Figure 4(b), we plot the normalized quantity $\langle\delta\nu_{02}\rangle/\langle\Delta\nu_0\rangle$ that in main-sequence stars is known to depend mostly on central physical conditions (Roxburgh & Vorontsov 2003). It is worth noticing that we plotted $\langle\delta\nu_{02}\rangle$ for models with different chemical compositions and convection treatment, nevertheless, a predominant dependence on mass and radius appears. For a given mass $\langle\delta\nu_{02}\rangle/\langle\Delta\nu_0\rangle$ increases with density contrast, i.e., as the star expands with smaller values of $\langle\nu_0\rangle$, decreases as the mass increases, and does not change significantly during the core He-B phase.

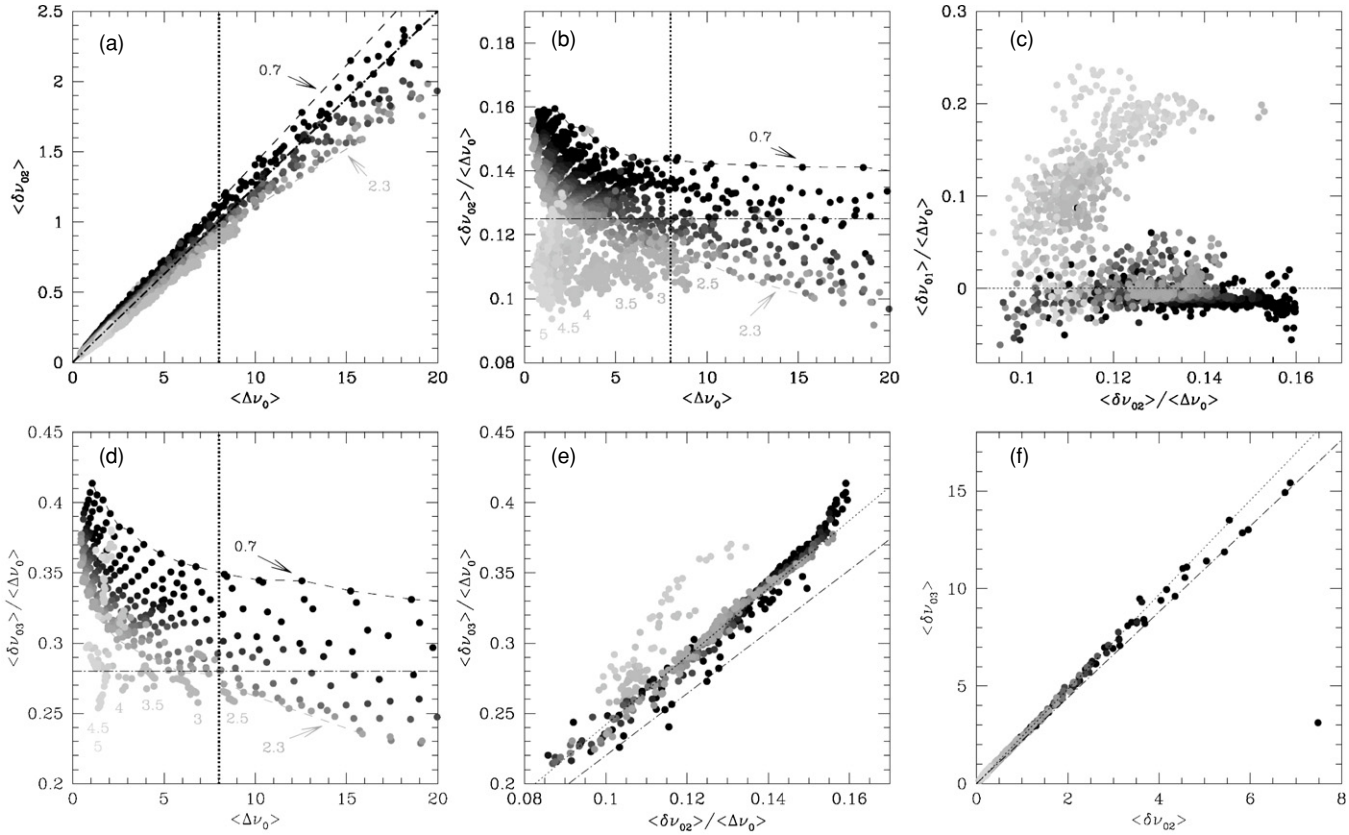

Figure 4. Small frequency separations for models with masses between 0.7 and 5 $M_{\odot}$ (each gray level corresponds to a different mass, from the darkest for 0.7 $M_{\odot}$ to the lightest for 5 $M_{\odot}$), $Z = 0.006$, 0.015, 0.02, and 0.03, $Y = 0.025$ and 0.278, and $\alpha_{\rm MLT} = 1.6$ and 1.9. Dotted vertical line indicates the minimum $\langle\Delta\nu\rangle$ from the first 34 days of *KEPLER* data and the dot-dashed lines correspond to the linear fits for these data from Bedding et al. (2010). (a) $\langle\delta\nu_{02}\rangle$ as a function of $\langle\Delta\nu_0\rangle$, for low-mass models (0.7–2.3 $M_{\odot}$) from the bottom of the RGB up to $\log L/L_{\odot}$ 2.5–3 $M_{\odot}$ and 2.5–5 $M_{\odot}$ models in the He-B phase (Y_c between 0.9 and 0.1). (b) Same as (a) but for the $\langle\delta\nu_{02}\rangle/\langle\Delta\nu_0\rangle$. (c) $\langle\delta\nu_{01}\rangle/\langle\Delta\nu_0\rangle$ as a function of $\langle\delta\nu_{02}\rangle/\langle\Delta\nu_0\rangle$ for the same models as in (a) and (b). Note the high concentration of RGB models with small and negative value of $\langle\delta\nu_{01}\rangle/\langle\Delta\nu_0\rangle$. (d) $\langle\delta\nu_{03}\rangle/\langle\Delta\nu_0\rangle$ vs. $\langle\Delta\nu_0\rangle$ for models with $Y = 0.278$, $Z = 0.02$, and $\alpha_{\rm MLT} = 1.9$. (e) $\langle\delta\nu_{03}\rangle/\langle\Delta\nu_0\rangle$ vs. $\langle\delta\nu_{02}\rangle/\langle\Delta\nu_0\rangle$ and models used in (d). (f) $\langle\delta\nu_{03}\rangle$ as a function of $\langle\delta\nu_{02}\rangle$ and models in (d).

In Figures 4(a) and (b), a vertical dotted line indicates the lower limit of $\langle\Delta\nu\rangle$ measured from the first 34 days of *KEPLER* mission and the dot-dashed line corresponds to the fit $\langle\delta\nu_{02}\rangle = 0.122\langle\Delta\nu_0\rangle$ proposed by Bedding et al. (2010) for those observations. The comparison between our figures and Figure 4 in Bedding et al. (2010) indicates that the predictions from theoretical models of low-mass stars (1–1.5 $M_{\odot}$) in the low luminosity part of the ascending RGB are consistent with observational data, as the scaling based on $\nu_{\rm max}$ and $\Delta\nu$ also suggests. In that paper, the authors also report the detection of $\ell = 3$ modes, and because of the scatter of $\ell = 1$ mode frequencies, they suggest to use a new small separation $\delta\nu_{03}(n) = 0.5\,(\nu_{0\,n-1} - 2\,\nu_{3\,n-2} + \nu_{0\,n})$ instead of the classic $\delta\nu_{13}$. Note that the observational data provide a ratio $\delta\nu_{03}/\delta\nu_{02} \sim 2.2$ (Bedding et al. 2010) instead of 2, which was predicted by the asymptotic theory. In the bottom panels of Figure 4, we plot the theoretical results for $\delta\nu_{03}$ and its relation with $\Delta\nu_0$ and $\delta\nu_{02}$. Bedding et al. (2010) results are represented by a dash-dotted line while the dotted line corresponds to our fit $\delta\nu_{03} \sim 2.42\,\delta\nu_{02}$. The dependence of $\delta\nu_{03}$ on stellar mass and radius is similar to that of $\delta\nu_{02}$, therefore no additional information should be expected from $\delta\nu_{03}$.

The small frequency separation $\delta\nu_{01}(n) = 0.5\,(\nu_{0n} - 2\,\nu_{1,n} + \nu_{0\,n+1})$ in main-sequence stars is also known to be sensitive to the center physical conditions. The asymptotic theory predicts a $\langle\delta\nu_{01}\rangle = 1/3\langle\delta\nu_{02}\rangle$ relationship. As it is evident in Figure 4(c), the "*p*-mode" spectrum for red giant models does not follow those predictions. In particular, a large number of models have negative or very small values of $\langle\delta\nu_{01}\rangle$ independently of $\langle\delta\nu_{02}\rangle$. Similar values of $\langle\delta\nu_{01}\rangle$ have also been found in the *KEPLER* data (Bedding et al. 2010) and in the oscillation spectrum of the *CoRoT* red giant HR 7349 (Carrier et al. 2010). We note that the largest concentration of negative/small $\langle\delta\nu_{01}\rangle$ values correspond to models ascending or descending the RGB. $\langle\delta\nu_{01}\rangle/\langle\Delta\nu\rangle$ versus luminosity confirms this result.

Searching for a common characteristic in the structure of these models, we find that while ascending and descending the RGB the turning points of $\ell = 1$ modes are well inside the convective envelope. The steady He-B models have a shallower convective envelope and the turning points of $\ell = 1$ modes are inside the radiative region. Figure 5(a) shows the variation of $\langle\delta\nu_{01}\rangle/\langle\Delta\nu\rangle$ with the distance (in acoustic radius $\tau(r') = \int_0^{r'} dr/c$) between the bottom of the convective zone (BCZ) and the turning point for a $\ell = 1$ mode with frequency close to $\nu_{\rm max}$ (tp_1). In Figure 5(b), we highlight the behavior of $\langle\delta\nu_{01}\rangle$ for low-mass RGB models. The scatter of $\langle\delta\nu_{01}\rangle/\langle\Delta\nu\rangle$ rapidly decreases as $\tau_{tpl_1} - \tau_{\rm BCZ}$ increases (deep convective envelope) and $\langle\delta\nu_{01}\rangle/\langle\Delta\nu\rangle$ takes negative values for models in which tp_1 is well inside the convective envelope.

4. CONCLUDING REMARKS

We presented the properties of the theoretical spectrum of solar-like oscillations during the RGB and core He-B phases of

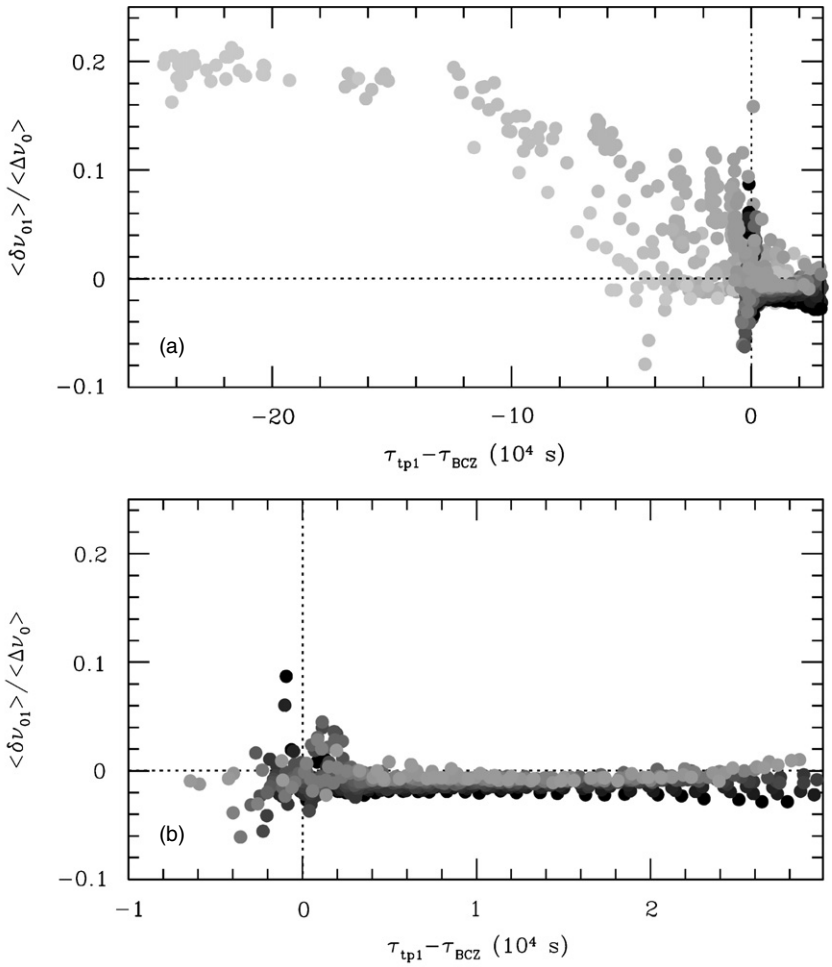

Figure 5. (a) $\langle \delta\nu_{01} \rangle / \langle \Delta\nu_0 \rangle$ as a function of the distance in acoustic radius between the bottom of the convective envelope $\tau_{\rm BCZ}$ and the $\ell = 1$ turning point $\tau_{\rm tp1}$ for models with $Z = 0.02$, $Y = 0.278$, $\alpha_{\rm MLT} = 1.9$, and masses between 0.7 and 5 $M_\odot$. (b) Zoom for low-mass models (0.7–2.3 $M_\odot$) in the RGB. Same gray level criteria as in Figure 4.

red giant evolution and analyzed the behavior of large and small frequency separations computed from modes well trapped in the acoustic cavity of these stars. The main results of this global overview are the following.

1. Independently of the evolutionary state, $\ell = 2$ and $\ell = 3$ modes trapped in the acoustic cavity have an inertia of the same order as that of the corresponding radial mode and behave as "*p*-modes" with frequencies regularly spaced by $\langle \Delta\nu \rangle$. As a consequence, the scatter of $\ell = 2$ modes in the folded échelle diagrams is rather small.
2. The trapping of $\ell = 1$ modes in the acoustic cavity depends on the evolutionary state. While a regular pattern of dipole modes is expected in more centrally condensed models ascending the RGB, the scatter significantly increases for core He-B ones. Therefore, the regularity of the $\ell = 1$ spectrum could be used to discriminate between different evolutionary phases.
3. $\langle \delta\nu_{02} \rangle$ and $\langle \delta\nu_{03} \rangle$ depend almost linearly on the large separation, hence on the mean density of the model, with a slope that slightly depends on the stellar mass.
4. $\langle \delta\nu_{01} \rangle$ seems to reflect the distance between the $\ell = 1$ turning point and the bottom of convective envelope. It takes negative (or small) values if tp_1 is well inside the convective envelope, as it occurs in models ascending or descending the RGB.
5. The properties of our adiabatic spectra are in good agreement with those found in *KEPLER* data for low-luminosity RGB stars (Bedding et al. 2010) and also with those for *CoRoT* exofield red giants. In this study, we predict a large scatter of dipole modes for "red clump" stars ($\Delta\nu \sim 4\ \mu$Hz; Hekker et al. 2009; Mosser et al. 2010a; Miglio et al. 2009b) as well as a regular pattern of $\ell = 0$ and 2 modes for all the red giants. Both features correspond quite well with the properties of the spectra found by Mosser et al. (2010b) in the *CoRoT* exofield red giants (see Figure 3 and their Figure 3).

J.M. and A.M. acknowledge financial support from the Prodex-ESA Contract Prodex 8 COROT (C90199) and FNRS. The authors thank M.A. Dupret for useful suggestions concerning oscillation frequency computations.

REFERENCES

Baglin, A., et al. 2002, in Stellar Structure and Habitable Planet Finding, ed. B. Battrick et al. (ESA SP-485; Noordwijk: ESA), 17
Barban, C., et al. 2007, A&A, 468, 1033
Bedding, T. R., et al. 2010, ApJ, 713, L176
Brown, T. M., Gilliland, R. L., Noyes, R. W., & Ramsey, L. W. 1991, ApJ, 368, 599
Canuto, V. M., Goldman, I., & Mazzitelli, I. 1996, ApJ, 473, 550

Carrier, F., et al. 2010, A&A, 509, A73
Christensen-Dalsgaard, J. 1988, in IAU Symp. 123, Advances in Helio- and Asteroseismology, ed. J. Christensen-Dalsgaard & S. Frandsen (Cambridge: Cambridge Univ. Press), 295
Christensen-Dalsgaard, J. 2004, Sol. Phys., 220, 137
De Ridder, J., et al. 2006, A&A, 448, 689
De Ridder, J., et al. 2009, Nature, 459, 398
Dupret, M., et al. 2009, A&A, 506, 57
Dziembowski, W. A., Gough, D. O., Houdek, G., & Sienkiewicz, R. 2001, MNRAS, 328, 601
Frandsen, S., et al. 2002, A&A, 394, L5
Girardi, L., Groenewegen, M. A. T., Hatziminaoglou, E., & da Costa, L. 2005, A&A, 436, 895
Gough, D. O. 1986, in Hydrodynamic and Magnetodynamic Problems in the Sun and Stars, ed. Y. Osaki (Tokyo: Univ. Tokyo Press), 117
Hekker, S., et al. 2009, A&A, 506, 465
Houdek, G., & Gough, D. O. 2002, MNRAS, 336, L65
Kjeldsen, H., & Bedding, T. R. 1995, A&A, 293, 87
Michaud, G., Richer, J., & Richard, O. 2010, A&A, 510, A104
Miglio, A., Montalbán, J., Eggenberger, P., Hekker, S., & Noels, A. 2009a, in AIP Conf. Ser. 1170, Stellar Pulsation: Challenges for Theory and Observation, ed. J. A. Guzik & P. A. Bradley (Melville, NY: AIP), 132
Miglio, A., et al. 2009b, A&A, 503, L21
Mosser, B., et al. 2010a, A&A, 517, 22
Mosser, B., et al. 2010b, A&A, submitted
Roxburgh, I. W., & Vorontsov, S. V. 2003, A&A, 411, 215
Scuflaire, R., et al. 2008, Ap&SS, 316, 149
Tassoul, M. 1980, ApJS, 43, 469
Vandakurov, Y. V. 1967, Astron. Zh., 44, 786
Ventura, P., D'Antona, F., & Mazzitelli, I. 2008, Ap&SS, 316, 93